

Internal correction of spectral interferences and mass bias for selenium metabolism studies using enriched stable isotopes in combination with multiple linear regression

Kristoffer Lunøe · Justo Giner Martínez-Sierra ·
Bente Gammelgaard · J. Ignacio García Alonso

Received: 13 October 2011 / Revised: 12 January 2012 / Accepted: 13 January 2012 / Published online: 10 February 2012
© Springer-Verlag 2012

Abstract The analytical methodology for the *in vivo* study of selenium metabolism using two enriched selenium isotopes has been modified, allowing for the internal correction of spectral interferences and mass bias both for total selenium and speciation analysis. The method is based on the combination of an already described dual-isotope procedure with a new data treatment strategy based on multiple linear regression. A metabolic enriched isotope (^{77}Se) is given orally to the test subject and a second isotope (^{74}Se) is employed for quantification. In our approach, all possible polyatomic interferences occurring in the measurement of the isotope composition of selenium by collision cell quadrupole ICP-MS are taken into account and their relative contribution calculated by multiple linear regression after minimisation of the residuals. As a result, all spectral interferences and mass bias are corrected internally allowing the fast and independent quantification of natural abundance selenium ($^{\text{nat}}\text{Se}$) and enriched ^{77}Se . In this sense, the calculation of the tracer/tracee ratio in each sample is straightforward. The method has been applied to study the time-related tissue incorporation of ^{77}Se in male Wistar rats while maintaining the $^{\text{nat}}\text{Se}$ steady-state conditions. Additionally, metabolically relevant information such as selenoprotein synthesis and selenium elimination in urine could be studied using the proposed methodology. In this case, serum proteins were separated by affinity chromatography while reverse phase

was employed for urine metabolites. In both cases, ^{74}Se was used as a post-column isotope dilution spike. The application of multiple linear regression to the whole chromatogram allowed us to calculate the contribution of bromine hydride, selenium hydride, argon polyatomics and mass bias on the observed selenium isotope patterns. By minimising the square sum of residuals for the whole chromatogram, internal correction of spectral interferences and mass bias could be accomplished. As a result, the tracer/tracee ratio could be calculated for each selenium-containing species and a time relationship for synthesis and degradation established. Both selenite and selenized yeast labelled with ^{77}Se were employed for comparative purposes.

Keywords Mass spectrometry · ICP-MS · Speciation · Biological samples

Introduction

Selenium is both an essential and a toxic element and has furthermore shown cancer-protective properties. Neither the mechanisms behind the cancer-protective properties nor the general metabolism are fully elucidated yet. The chemical forms of selenium are of key importance and speciation studies are therefore needed to gather knowledge as to the species transformation occurring in the organism; selenium speciation and metabolism have recently been reviewed [1].

Studies aimed at clarifying the selenium metabolism and cancer-protective effect need the ability to trace the selenium from administration to excretion. By use of enriched stable isotopes, radioactive tracers, formerly employed for this type of study, are avoided. Enriched stable isotopes of selenium have been employed by different research groups [2–9] both for the total determination and speciation analysis of selenium

K. Lunøe · B. Gammelgaard
Department of Pharmaceutics and Analytical Chemistry,
Faculty of Pharmaceutical Sciences, University of Copenhagen,
2100 Copenhagen, Denmark

J. G. Martínez-Sierra · J. I. G. Alonso (✉)
Department of Physical and Analytical Chemistry,
University of Oviedo,
33006 Oviedo, Spain
e-mail: jiga@uniovi.es

in biological materials and/or for metabolism purposes [10–14]. In most cases, final quantitative measurements are performed by ICP-MS using a collision/reaction cell instrument. The accurate determination of total selenium in biological materials by isotope dilution analysis has been described [1]. Additionally, speciation methodologies combining affinity separations and post-column isotope dilution analysis were developed [2] and further improved [3–6] for the determination of Glutathione peroxidase (GPX3), Selenoprotein P (SePP1) and Selenoalbumin (SeAlb) in blood serum. For *in vivo* metabolism studies, two general isotopic procedures were described: (a) the saturation of the animals with an enriched isotope of selenium [10–14] or (b) the use of a double isotope procedure without prior isotopic saturation [8, 9]. In all cases, severe polyatomic interferences from bromine hydride (BrH), selenium hydride (SeH) and argon polyatomics (Ar_2 and Ar_2H) needed to be corrected for. Generally, external correction based on natural abundance bromine or selenium standards was employed for the elimination of spectral interferences [2, 3, 8, 9]. So, the SeH/Se and the BrH/Br factors were measured externally and applied for the correction in the measured samples. Rodriguez-Castrillon *et al.* [15] showed that the values of SeH/Se and BrH/Br in the real samples could be different from those measured in the standards and developed an internal correction procedure in the determination of total selenium in biological materials based on multiple linear regression. However, the method was developed for total determinations and when only one enriched isotope of selenium was employed. For speciation analysis in metabolic studies, and when more than one enriched isotopes were used, the classical external correction procedure was applied [8]. In the paper of Gonzalez-Iglesias *et al.* [8] for selenium speciation in urine samples, the bromine peak eluted at the same time as the inorganic selenium peak. Under those circumstances a very good estimation of the BrH/Br factor is required because slight over- or under-correction of the interference will provide variable signals of the inorganic selenium peak at mass 80. So, it is important to calculate the correction factors to be applied in the real samples and not in standard solutions as those have been observed to change [15]. Also, the internal correction procedure is much faster than the previous method as it not requires the measurement of any external standard.

In this paper, we extend the internal correction procedure developed by Rodriguez-Castrillon *et al.* [15] for selenium metabolic studies including speciation analysis and when two selenium enriched isotopes are used. The multiple linear regression procedure allows the automatic and internal correction of all possible spectral interferences (BrH, SeH, Ar_2 , Ar_2H) and the calculation of the instrumental mass bias to be applied for the correction of the selenium isotope abundances. The method was developed for the case when two enriched isotopes of selenium are employed (^{77}Se as metabolic tracer and ^{74}Se as

quantitation tracer) both for total selenium determination in biological fluids and tissues and for speciation studies in blood serum and urine. To illustrate the advantages of the proposed procedure the method was applied for the study of the time related tissue incorporation and selenoprotein synthesis in male Wistar rats fed with ^{77}Se -enriched selenite and selenized yeast.

Experimental

Instrumentation

The ICP-MS used was an Agilent 7500ce (Agilent Technologies, Kyoto, Japan). For interference suppression, the collision cell was employed in the helium mode with 4 mL/min He. Other relevant operating parameters are given in Table 1. Masses measured were 74, 75, 76, 77, 78, 79, 80, 81, 82 and 83 for all samples. Speciation analyses were performed with a Shimadzu LC-20AD UFLC system (Shimadzu, Duisburg, Germany) comprising two LC pumps and a system controller directly coupled to the nebulizer of the ICP-MS instrument. Tissue samples were digested using a microwave oven from CEM (Matthews, North Carolina, USA). All sample preparation was done gravimetrically.

Reagents and materials

Enriched isotopes of selenium ^{74}Se and ^{77}Se were obtained in solid form from Cambridge Isotope Laboratories (Andover, MA, USA) and dissolved in nitric acid. These selenium standards were in the form of Se(IV) and were already characterised in isotope composition and concentration [8, 9]. Selenized yeast labelled with ^{77}Se was generously supplied by PharmaNord (Vejle, Denmark). This selenized yeast has been previously characterised both in isotopic composition and selenium concentration [16]. The isotope composition of all enriched isotopes employed together with the natural selenium abundance is included in Table 2. Please note that the isotopic composition of the inorganic and yeast ^{77}Se was slightly different.

Table 1 Typical operating parameters for the ICP-MS used for the selenium measurements

Agilent 7500ce ICP-MS		
Parameter	Value	Unit
RF Power	1,500	W
Carrier Gas	1.15	L/min
QP Focus	-10	V
QP Bias	-16	V
OctP Bias	-18	V
He Gas	4	mL/min

Table 2 Selenium isotopic patterns used in the calculations for natural abundance selenium (^{nat}Se), ^{74}Se enriched selenium (^{74}Se) and ^{77}Se enriched selenium (^{77}Se) both as labelled yeast or inorganic selenium

Mass	^{nat}Se	^{74}Se	^{77}Se (yeast)	^{77}Se (inorganic)
74	0.0089	0.9967	0.0003	0.0006
76	0.0937	0.0006	0.0007	0.0103
77	0.0763	0.0003	0.9933	0.911
78	0.2377	0.0007	0.002	0.039
79	0.0000	0.0000	0.0000	0.0000
80	0.4961	0.0015	0.002	0.034
81	0.0000	0.0000	0.0000	0.0000
82	0.0873	0.0003	0.002	0.0054
83	0.0000	0.0000	0.0000	0.0000

Animal experiments

Animal experiments were carried out following the guidelines established by The Animal Experiments Directive (86/609/EEC) on the protection of animals used for experimental and other scientific purposes. Male Wistar rats were kept in separate metabolic cages and exposed to 12-h light–dark cycles. A number of 11 rats were employed in this experiment. Rats were fed *ca.* 10 μg of ^{77}Se either as selenite or selenized yeast and faeces and urine samples were collected after 0, 6, 12, 18, 24 and 48 h. Drinking water and standard maintenance feed were available *ad libitum*. At each time interval, a corresponding ^{77}Se labelled rat from each group was anesthetized using an isoflurane–oxygen mixture and the blood extracted by heart puncture. Afterwards the rats were killed by severing the spinal cord. Different tissues (brain, testes, kidney, spleen, pancreas–intestine, liver, lungs and heart) were collected.

Sample preparation

For tissue samples representative, accurately weighed (wet weight) cuts from the extracted tissue were taken and these were microwave digested in 1 mL sub-boiled nitric acid. Total selenium determination was carried out after spiking with a known amount of ^{74}Se . The blood of the rat was allowed to clot and afterwards centrifuged 5 min at 3,000 rpm, the supernatant transferred to a clean tube and centrifuged again. The resulting supernatant was portioned out in Eppendorf tubes and frozen at $-20\text{ }^{\circ}\text{C}$ until analysis. The serum was diluted 1+1 with mobile phase A before injection. The red blood cells were digested as for the tissue samples. The urine samples were centrifuged and the supernatant portioned into Eppendorf tubes and frozen at $-20\text{ }^{\circ}\text{C}$ until analysis. Faeces samples were digested as for tissue samples.

Chromatographic procedures

For serum speciation, the affinity chromatography setup was an adapted version of the method originally developed by Reyes *et al.* [2] and since refined by Jitaru *et al.* [4–7]. The applied method made use of unmodified 1 mL HiTrap[®] Blue and 1 mL HiTrap[®] Heparin columns (GE Healthcare, Barcelona, Spain). Mobile phase A was 0.05 mol/L ammonium acetate and mobile phase B was 1.5 mol/L ammonium acetate. Injection volume was 100 μL . The post-column isotope dilution solution was 20 ng/g ^{74}Se in 1% HNO_3 and was introduced into the LC flow at 0.3 g/min by a peristaltic pump. For urine speciation we employed the same reverse phase chromatography setup used by González Iglesias *et al.* [8] and the same post-column spike used for the affinity separation. An injection volume of 50 μL was employed for the urine analysis.

Data treatment procedures

Two data treatment procedures based on multiple linear regression were developed either for total selenium analysis or speciation analysis. It was assumed that all intensities measured were originating from five different isotopic signatures in the sample: natural abundance selenium (^{nat}Se), ^{77}Se labelled selenium (^{77}Se) used as metabolic tracer, ^{74}Se labelled selenium (^{74}Se) added for quantification, natural abundance bromide (^{nat}Br) present in all samples and natural abundance argon (^{nat}Ar) present as polyatomic interferences not completely eliminated by the collision cell. The theoretical isotope signatures employed were calculated taking into account the possible formation of hydrides for all components. For selenium, a single SeH/Se factor was applied to all isotopic signatures considered. For total selenium analysis, the raw intensity data at masses 74, 76, 77, 78, 79, 80, 81, 82 and 83 were first corrected for mass bias using the exponential mass bias correction equation:

$$I_i = I_i^{\text{exp}} e^{-k\Delta M} \quad (1)$$

Where I_i are the corrected intensities and I_i^{exp} the measured intensities. The mass bias factor k was given an initial value of 0 and was then optimised by the least square procedure. All ΔM values were the nominal mass differences *versus* mass 80 of selenium which was used as reference. Then, all corrected intensities were converted into relative abundances, A_i , using the equation:

$$A_i = \frac{I_i}{\sum_{i=74}^{i=83} I_i} \quad (2)$$

These relative abundances were subjected to multiple linear regression using the five component isotope matrix

corresponding to ^{nat}Se , ^{77}Se , ^{74}Se , ^{nat}Br and ^{nat}Ar . Finally, the residuals of the multiple linear regression were minimised by changing the mass bias factor, k , and the SeH/Se , BrH/Br and $\text{Ar}_2\text{H}/\text{Ar}_2$ factors employed to calculate the theoretical isotope abundances in the multiple linear regression. For this purpose, the SOLVER application in Excel was used. As a result, the molar fractions and their uncertainties corresponding to the three selenium isotope signatures in the sample were calculated. The concentrations of ^{nat}Se and ^{77}Se were then calculated using the equations:

$$N_{nat\text{Se}} = N_{74\text{Se}} \frac{X_{nat\text{Se}}}{X_{74\text{Se}}} \quad (3)$$

and

$$N_{77\text{Se}} = N_{74\text{Se}} \frac{X_{77\text{Se}}}{X_{74\text{Se}}} \quad (4)$$

Where N_{nat} , N_{74} and N_{77} are the moles of natural abundance selenium and selenium enriched in either ^{74}Se or ^{77}Se , respectively. The known weights of sample and spike taken together with the corresponding atomic weights then enable the calculation of the individual concentrations.

For speciation analysis, a similar procedure was employed. First, all intensities in the chromatogram were corrected for mass bias as indicated above. For every time interval, a multiple linear regression calculation was performed and a “reconstructed” chromatogram was calculated for all masses. The intensity differences between the experimental chromatogram and the reconstructed chromatogram are the residuals at each mass. The sum of squared residuals was then calculated for all measured masses and for the whole chromatogram and minimised by changing the mass bias and the hydride factors. As a result, the molar fractions for ^{nat}Se , ^{77}Se and ^{74}Se were obtained. From those molar fractions, a relative molar flow chromatogram was obtained. The integration of the peaks in the molar flow chromatogram produced the amounts of ^{nat}Se and ^{77}Se in the corresponding peaks as explained previously [8, 9].

Results and discussion

Development of the calculation procedure for total selenium determination

The measurement of selenium isotopes by ICP-MS is hindered by several spectral interferences. Argon polyatomics (Ar_2^+ and Ar_2H^+) are present mainly at masses

76, 78, 80 and 81 while bromine hydrides affect masses 80 and 82 of selenium. Additionally, selenium can also form hydrides which will be observed as low signals at masses 75, 77, 78, 79, 81 and 83. Argon polyatomics can be reduced or even eliminated in collision cell quadrupole instruments by using helium, hydrogen or mixtures of both as collision gas [2, 3]. Dynamic Reaction Cell quadrupole instruments most often use methane as reaction gas to eliminate the polyatomic argon interferences [16–18]. Bromine and selenium hydrides cannot be eliminated by the cell technologies and their contribution needs to be corrected for. When performing isotopic measurements on selenium, these spectral interferences are usually corrected by an external procedure in which bromine and selenium standards are used to calculate the BrH/Br and SeH/Se factors [2, 3, 8, 9]. However, it has been observed that these factors may not be the same for samples and standards and an internal correction procedure based on multiple linear regression was developed [15]. The internal correction procedure was only developed for a single enriched isotope of selenium and for total analysis. This procedure is extended here to metabolism studies both for total analysis and speciation where two enriched isotopes of selenium are considered: a metabolic isotope and a quantitation isotope. The internal correction procedure is particularly important when the retention time of the selenium species is similar to that of bromine as it occurs for inorganic selenium in urine samples and for Glutathione peroxidase in serum samples.

The procedure is based on multiple linear regression in which the intensities measured at masses 74, 76, 77, 78, 79, 80, 81, 82 and 83 are deconvoluted by multiple least squares into the molar fractions of five different isotope patterns. These five isotope patterns considered are those of natural abundance selenium (^{nat}Se), enriched ^{77}Se (^{77}Se), enriched ^{74}Se (^{74}Se), natural abundance bromine (^{nat}Br) and natural abundance argon (^{nat}Ar). The theoretical isotope patterns considered in the multiple linear regression fitting were those of the expected species in the plasma. For selenium, the theoretical patterns included the contribution of Se^+ and SeH^+ with a given SeH/Se ratio which was the same for all isotopic forms of selenium considered. For bromine the theoretical patterns included both Br^+ and BrH^+ at a given BrH/Br ratio. Finally, for argon the theoretical patterns included Ar_2^+ and Ar_2H^+ at a given $\text{Ar}_2\text{H}/\text{Ar}_2$ ratio. It was necessary to include the argon pattern to improve the fit of the multiple linear regression even when this contribution was small in the collision cell instrument. We did not consider the possibility of ArCl interferences at masses 75 and 77 as these are readily removed by the collision cell instrument.

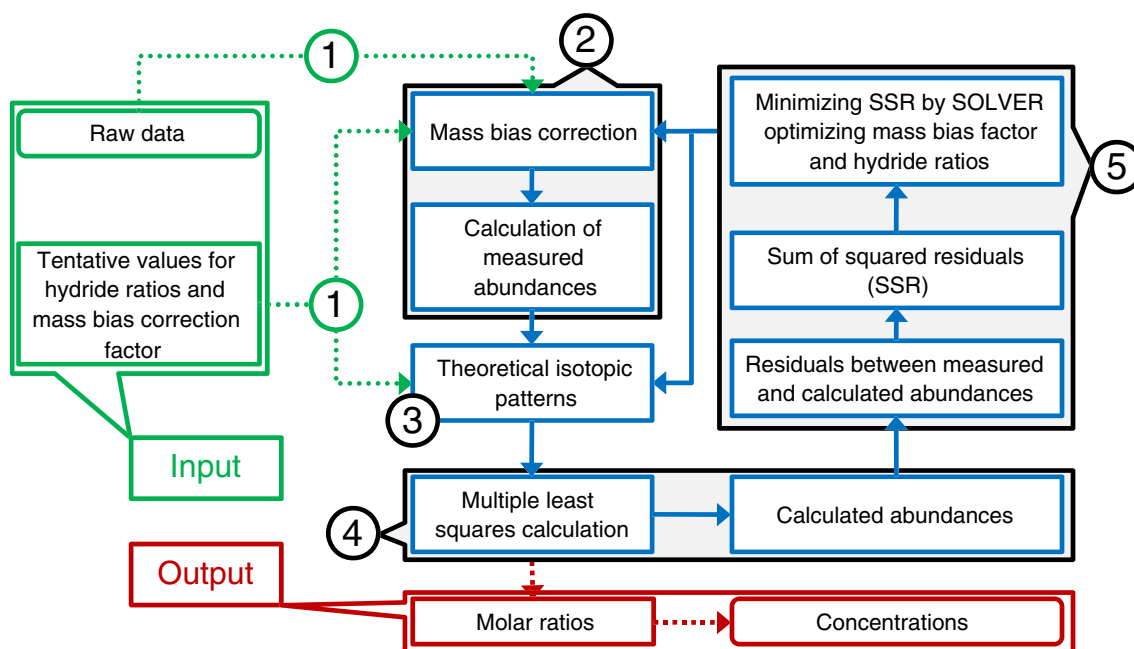


Fig. 1 Flow diagram of the calculation procedure. (1) Input raw data along with tentative values for hydride ratios and the mass bias correction factor (*k*). (2) Correct for mass bias using tentative *k* value and calculate abundances. (3) Calculate theoretical isotopic patterns based on tentative hydride ratios. (4) Apply multiple least squares

calculations and find calculated abundances. (5) Calculate residuals between measured and calculated abundances and let the SOLVER function minimize the sum of squared residuals by changing the hydride ratios and mass bias

The multiple linear regression equation used is shown below:

$$\begin{bmatrix} A_{74} \\ A_{76} \\ A_{77} \\ A_{78} \\ A_{79} \\ A_{80} \\ A_{81} \\ A_{82} \\ A_{83} \end{bmatrix} = \begin{bmatrix} A_{74}^{natSe} & A_{74}^{77Se} & A_{74}^{74Se} & A_{74}^{natBr} & A_{74}^{natAr} \\ A_{76}^{natSe} & A_{76}^{77Se} & A_{76}^{74Se} & A_{76}^{natBr} & A_{76}^{natAr} \\ A_{77}^{natSe} & A_{77}^{77Se} & A_{77}^{74Se} & A_{77}^{natBr} & A_{77}^{natAr} \\ A_{78}^{natSe} & A_{78}^{77Se} & A_{78}^{74Se} & A_{78}^{natBr} & A_{78}^{natAr} \\ A_{79}^{natSe} & A_{79}^{77Se} & A_{79}^{74Se} & A_{79}^{natBr} & A_{79}^{natAr} \\ A_{80}^{natSe} & A_{80}^{77Se} & A_{80}^{74Se} & A_{80}^{natBr} & A_{80}^{natAr} \\ A_{81}^{natSe} & A_{81}^{77Se} & A_{81}^{74Se} & A_{81}^{natBr} & A_{81}^{natAr} \\ A_{82}^{natSe} & A_{82}^{77Se} & A_{82}^{74Se} & A_{82}^{natBr} & A_{82}^{natAr} \\ A_{83}^{natSe} & A_{83}^{77Se} & A_{83}^{74Se} & A_{83}^{natBr} & A_{83}^{natAr} \end{bmatrix} \times \begin{bmatrix} x_{natSe} \\ x_{77Se} \\ x_{74Se} \\ x_{natBr} \\ x_{natAr} \end{bmatrix} + \begin{bmatrix} e_{74} \\ e_{76} \\ e_{77} \\ e_{78} \\ e_{79} \\ e_{80} \\ e_{81} \\ e_{82} \\ e_{83} \end{bmatrix} \tag{5}$$

The measured abundances at masses 74 to 83 are deconvoluted into five theoretical isotope patterns, *j*, and the contribution of each isotope pattern to the observed abundances, *x_j*, calculated. As we have more equations (*i*=9) than unknowns (*j*=5), we have to include an error vector in the equation. The squared sum of all *e_i* values is the square sum of residuals of the multiple linear regression. This square sum of residuals is important as it can be employed for the correction of systematic errors in the regression such as spectral interferences or mass bias [15].

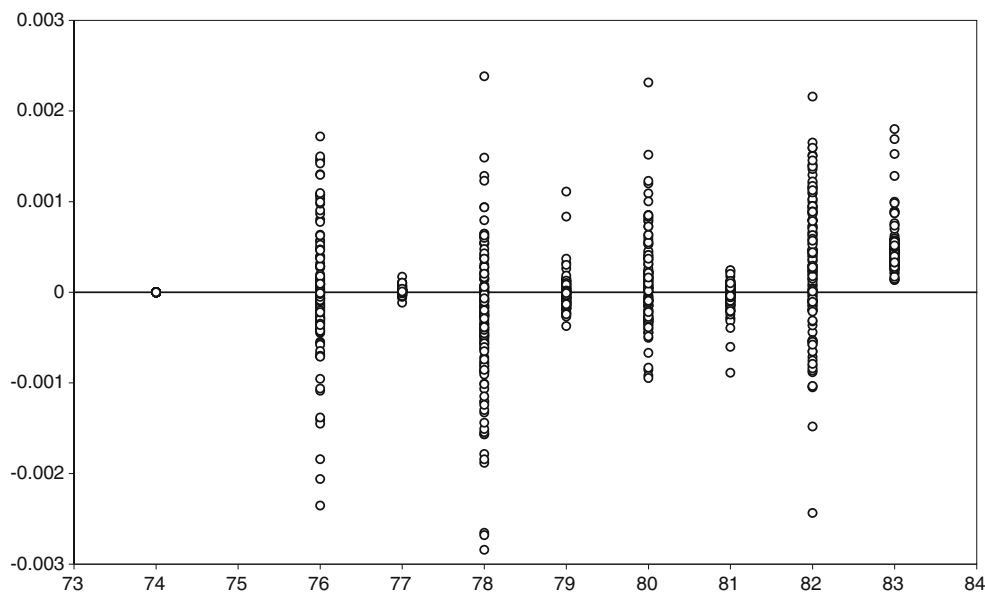
An important source of systematic errors in multiple linear regression is mass bias. The transport and detection efficiency of different isotopes of an element normally increases with mass in ICP-MS. So, when fitting several theoretical isotope patterns to one observed convoluted pattern the effect of mass bias needs to be considered. Mass bias is usually defined for a

single element. In this paper we have considered that the different transmission of all measured masses (arising either from Se, Br or Ar species) could be modelled with a single mass bias factor. So, the original intensities measured were corrected for mass bias using Eq. (1) regardless of the originating species. The reference isotope was taken as mass 80 for convenience but any other isotope could have been taken without affecting the results. Once mass bias corrected intensities are calculated, the measured isotope abundances to be used in Eq. (5) are determined using Eq. (2): each corrected intensity is divided by the sum of all intensities.

Table 3 Example of the theoretical isotope patterns calculated for the five components after optimisation of the hydride factors. In this case SeH/Se=0.030, BrH/Br=0.128 and Ar₂H/Ar₂=4.06

Mass	Natural Se	⁷⁴ Se	⁷⁷ Se (yeast)	Natural Br	Natural Ar
74	0.00864	0.96782	0.00029	0.00000	0.00000
76	0.09099	0.00058	0.00068	0.00000	0.00132
77	0.07680	0.00031	0.96454	0.00000	0.00538
78	0.23302	0.00069	0.03072	0.00000	0.00025
79	0.00689	0.00002	0.00006	0.44944	0.00101
80	0.48173	0.00146	0.00194	0.05746	0.19595
81	0.01437	0.00004	0.00006	0.43721	0.79607
82	0.08477	0.00029	0.00194	0.05589	0.00000
83	0.00253	0.00001	0.00006	0.00000	0.00000

Fig. 2 Residuals of the multiple linear regression for the 132 samples analysed for total selenium determination



For the calculation of the multiple linear regression, it is important to take into account that the theoretical patterns to be used in Eq. (5) can be optimised as well. Depending on the SeH/Se , BrH/Br and $\text{Ar}_2\text{H/Ar}_2$ factors considered, different theoretical patterns can be generated. Obviously, the “right” hydride factors to be employed when building the theoretical patterns will be those producing a minimum in the sum of squared residuals of the multiple linear regression. If we take into account that, for each sample, five contribution factors, x_j , need to be calculated, and four parameters optimised, it was found necessary to gain degrees of freedom by assuming that the four parameters to be optimised (k , SeH/Se , BrH/Br and $\text{Ar}_2\text{H/Ar}_2$) remained

constant for the group of samples analysed on the same run. So, the minimisation of the sum of squared residuals was made for a group of samples rather than for individual samples. For example, for the 132 samples analysed on the same run, 664 parameters needed to be calculated ($5 \times 132 + 4$) with 1188 data points ($9 \text{ masses} \times 132$) resulting in 524 degrees of freedom. It was observed that the optimisation procedure using the SOLVER application in Excel was straightforward when many samples were optimised simultaneously.

The flow diagram of the calculation procedure employed is shown in Fig. 1. First, tentative values are given to the four parameters to be optimised for all samples: k , SeH/Se , BrH/Br

Fig. 3 Variation of the optimized hydride factors SeH/Se and BrH/Br (left axis) and the mass bias factor k (right axis) for the 11 serum samples analysed by LC-ICP-MS. Average and standard deviation values are also shown

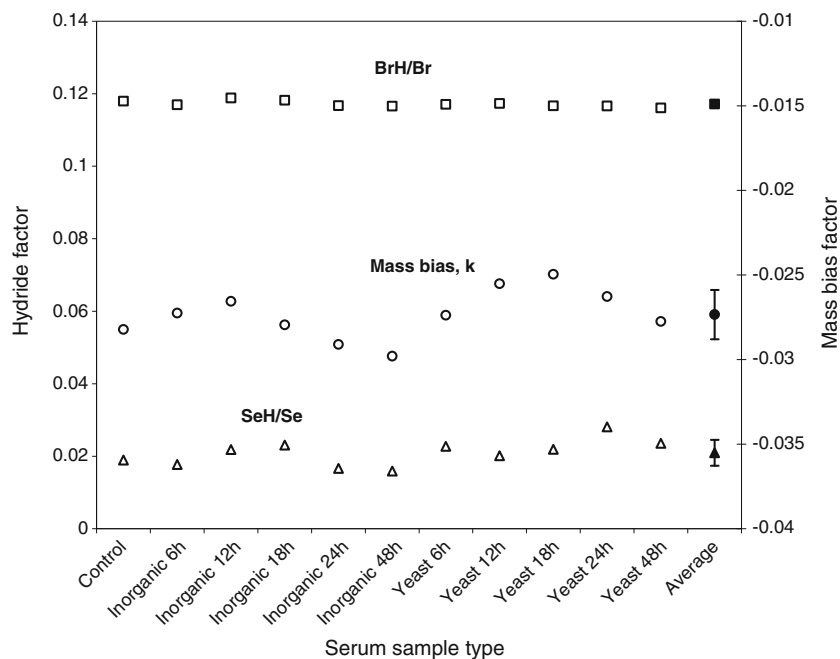


Fig. 4 Steps in the calculation for the affinity chromatographic method (6 h after yeast ^{77}Se administration), see the “Experimental” section for details. **(a)** Experimental (*red line*) and reconstructed (*black dashed line*) chromatograms at mass 80 together with the residuals obtained (*circles, right axis*). **(b)** Contribution factors for $^{\text{nat}}\text{Br}$, $^{\text{nat}}\text{Se}$, ^{77}Se and ^{74}Se . **(c)** Pattern-specific relative molar flow chromatogram

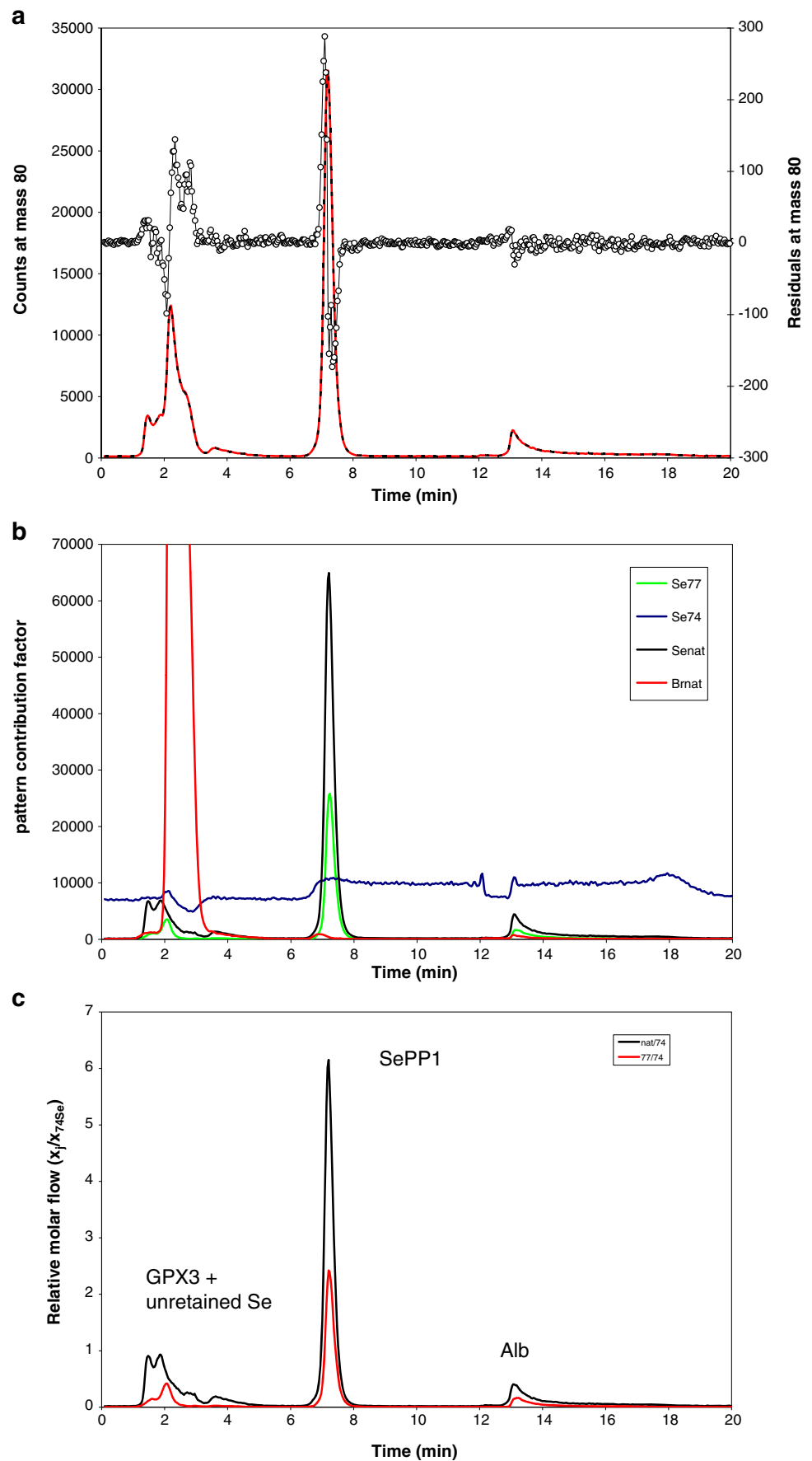


Table 4 Total selenium results obtained for the experiments with ^{77}Se in inorganic form

Sample	Control (76 g)		6 h (94 g)		12 h (143 g)		18 h (134 g)		24 h (135 g)		48 h (120 g)	
	$^{\text{nat}}\text{Se}$	^{77}Se	$^{\text{nat}}\text{Se}$	^{77}Se	$^{\text{nat}}\text{Se}$	^{77}Se	$^{\text{nat}}\text{Se}$	^{77}Se	$^{\text{nat}}\text{Se}$	^{77}Se	$^{\text{nat}}\text{Se}$	^{77}Se
Brain	134.5±1.3	-0.2±0.8	176.6±6.9	20.0±4.1	166.2±2.6	7.3±1.5	166.4±3.3	7.5±1.9	170.1±3.7	10.4±2.2	161.0±1.8	5.0±1.1
Testes	683.5±3.7	-1.6±2.1	543.2±4.1	41.7±2.4	687.0±7.9	23.4±4.6	561.0±9.0	29.8±5.3	584.5±8.9	38.0±5.2	717±12	38.3±6.9
Kidney	847±10	-3.2±5.5	869.4±4.9	444.4±2.9	730.0±6.0	247.9±3.4	825.5±5.3	241.2±3.1	778.3±8.8	211.7±5.1	867±10	134.1±5.7
Spleen	335.4±2.8	-2.7±2.8	350.3±5.8	115.0±3.4	325.7±4.2	44.9±2.5	313.9±5.3	65.4±3.1	334.6±3.7	50.8±2.2	416.0±7.6	47.7±4.5
Pancreas–intestine	303.1±4.1	-2.9±2.4	243.8±4.1	150.8±2.4	204.9±4.1	70.1±2.4	217.6±4.2	38.3±2.5	210.1±5.6	49.9±3.3	228.1±4.2	22.1±2.5
Liver	702.9±2.9	-2.8±1.7	556.5±9.4	532.3±5.6	781±12	336.0±7.2	512.9±6.8	132.3±4.0	573±10	116.2±5.8	535.9±9.4	69.3±5.5
Lungs	285.3±5.0	0.0±2.9	300.9±5.3	155.2±3.1	267.7±5.2	63.1±3.0	302±10	59.4±6.0	291.4±8.5	55.6±5.0	345±10	39.8±5.8
Heart	340.3±8.6	2.6±5.1	216.2±6.2	68.2±3.7	275.7±4.2	30.2±2.5	287.9±3.9	39.2±2.3	283.8±3.7	35.3±2.2	292.1±3.1	20.9±1.8
Red blood cells	331.7±8.2	-2.4±4.9	312.3±7.0	60.8±4.1	277.6±4.3	36.0±2.5	333.2±8.9	38.2±5.3	283.7±5.5	30.8±3.2	289.9±6.1	26.1±3.6
Serum	293.1±3.9	-0.8±2.1	223.3±2.3	122.3±1.3	244.6±1.9	97.6±1.1	237.3±1.2	90.8±0.7	247.3±3.3	75.4±1.9	291.6±2.6	51.7±1.5
Urine	63.2±1.6	-0.8±0.9	51.1±0.9	193.8±0.5	147.1±1.7	478.0±1.4	268.8±2.9	508.8±2.4	259.5±3.6	540.1±3.1	228.7±3.8	164.5±2.3
Faeces	111.1±9.0	0.0±5.3	109±10	6.6±5.7	134.3±6.6	37.9±3.9	149.8±7.8	183.3±4.6	129.1±5.8	255.8±3.4	141.2±5.0	23.0±2.9

Concentrations in ng/g wet weight except serum and urine. Uncertainties are indicated as standard uncertainties. The weights of the rats are indicated in parentheses

Br and $\text{Ar}_2\text{H}/\text{Ar}_2$. Second, the measured abundances in the samples are calculated using Eqs. (1) and (2). Third, the theoretical isotope patterns are computed based on the given SeH/Se , BrH/Br and $\text{Ar}_2\text{H}/\text{Ar}_2$ factors and, fourth, the contribution of the different components is calculated by multiple linear regression (function LINEST in Excel) using Eq. (5) for all samples considered. Finally, an iterative procedure is initiated (SOLVER in Excel) in which the sum of squared residuals, pooled for all samples considered, is minimised by changing the four correction parameters. Typical values of the theoretical isotope patterns generated taking into account

the hydride contribution are given in Table 3. Please compare these theoretical patterns generated taking into account the hydride contribution with the pure selenium isotope patterns given in Table 2 and those for bromine published by the IUPAC (0.5069 for ^{79}Br and 0.4931 for ^{81}Br) [19]. The observed hydride factors for SeH/Se and BrH/Br , 0.030 and 0.128 respectively, were typical of those determined in the same instrument [2, 3, 15].

Figure 2 shows the goodness of fit for the multiple linear regression. All residuals for the 132 samples measured are plotted for the different measured masses. As can be

Table 5 Total selenium results obtained for the experiments with ^{77}Se in organic form (yeast)

Sample	6 h (129 g)		12 h (161 g)		18 h (127 g)		24 h (90 g)		48 h (120 g)	
	$^{\text{nat}}\text{Se}$	^{77}Se	$^{\text{nat}}\text{Se}$	^{77}Se	$^{\text{nat}}\text{Se}$	^{77}Se	$^{\text{nat}}\text{Se}$	^{77}Se	$^{\text{nat}}\text{Se}$	^{77}Se
Brain	162.4±3.9	17.6±2.1	156.6±4.2	14.6±2.3	153.4±1.9	22.7±1.1	181.7±3.3	21.1±1.8	171.9±5.4	11.0±3.0
Testes	690.0±4.6	34.5±2.5	767.4±4.4	32.7±2.3	763.8±8.1	44.4±4.3	532.7±8.1	65.5±4.4	725.9±6.0	37.4±3.2
Kidney	822.4±5.0	225.3±2.7	945±10	262.8±5.1	829.0±9.3	282.4±5.0	850.0±7.0	254.3±3.8	910.8±6.7	140.8±3.6
Spleen	348.1±5.0	90.7±2.7	314.7±4.0	65.8±2.1	342±13	91.0±6.9	382.9±3.5	88.1±1.9	382.9±5.1	44.2±2.7
Pancreas–intestine	193.6±3.3	110.2±1.8	240.6±3.2	105.6±1.7	249.3±4.9	138.0±2.6	216.5±6.4	80.4±3.5	287.9±4.2	48.2±2.3
Liver	611.2±4.6	244.2±2.4	707.5±5.4	152.9±2.9	639.1±8.5	168.6±4.6	569.8±4.7	178.5±2.6	644.2±2.9	92.2±1.6
Lungs	338.9±5.4	86.6±2.9	244.6±8.1	54.9±4.4	290.0±8.1	84.5±4.4	305.2±7.4	75.3±4.0	317.8±3.7	37.8±2.0
Heart	293.2±3.1	40.1±1.7	274.1±4.4	32.1±2.4	291.1±2.1	50.7±1.1	305.8±7.5	48.4±4.1	295.0±2.1	24.9±1.1
Red blood cells	281.1±8.0	26.0±4.4	315.8±6.3	40.9±3.4	290±11	36.8±6.1	288.0±8.8	41.5±4.8	325±10	27.2±5.3
Serum	235.8±2.1	70.6±1.1	265.5±2.5	83.8±1.3	267.6±1.6	109.3±0.8	251.0±2.4	90.3±1.3	307.3±1.3	55.8±0.7
Urine	266.7±4.4	711.6±4.5	163.2±1.5	147.9±0.9	316.6±5.4	618.5±4.9	366.9±4.8	641.4±4.4	140.1±3.8	65.2±2.1
Faeces	118.9±5.9	-0.5±3.2	180.3±5.3	71.1±2.9	152.4±5.6	197.8±3.0	86.2±3.2	45.6±1.8	123.3±7.4	17.3±4.0

Concentrations in ng/g wet weight except serum and urine. Uncertainties are indicated as standard uncertainties. The weights of the rats are indicated in parentheses

observed, all residuals were lower than ± 0.003 and showed a uniform distribution between positive and negative values. No influence of the sample type (i.e. tissues, urine, blood, etc.) on the residual distribution was observed.

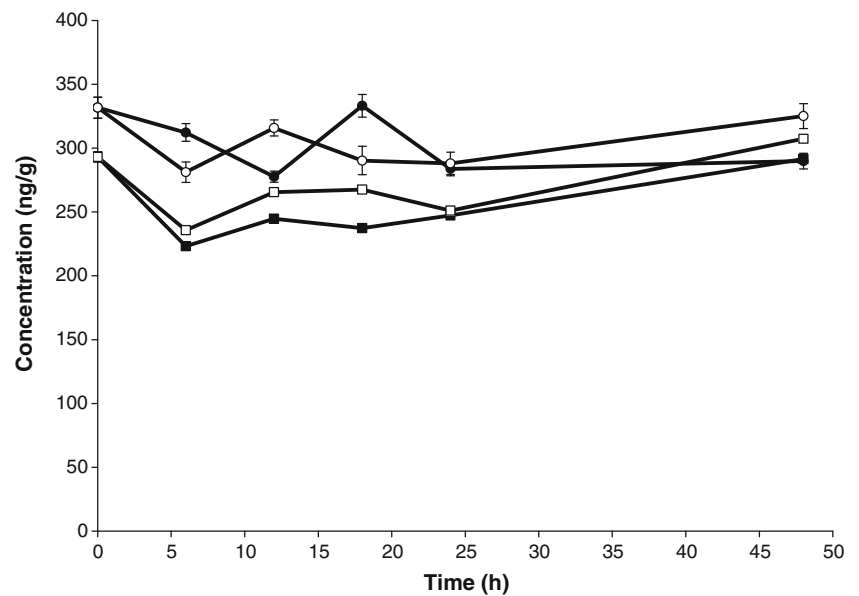
Once the contribution factors for ^{nat}Se ($x_{nat\text{Se}}$), ^{77}Se ($x_{77\text{Se}}$) and ^{74}Se ($x_{74\text{Se}}$) are calculated for all samples, Eqs. (3) and (4) are applied to compute independently the concentrations of ^{nat}Se and labelled ^{77}Se in all samples. The tracer/tracee ratio is obtained directly by the ratio $x_{77\text{Se}}/x_{nat\text{Se}}$.

Development of the calculation procedure for selenium speciation

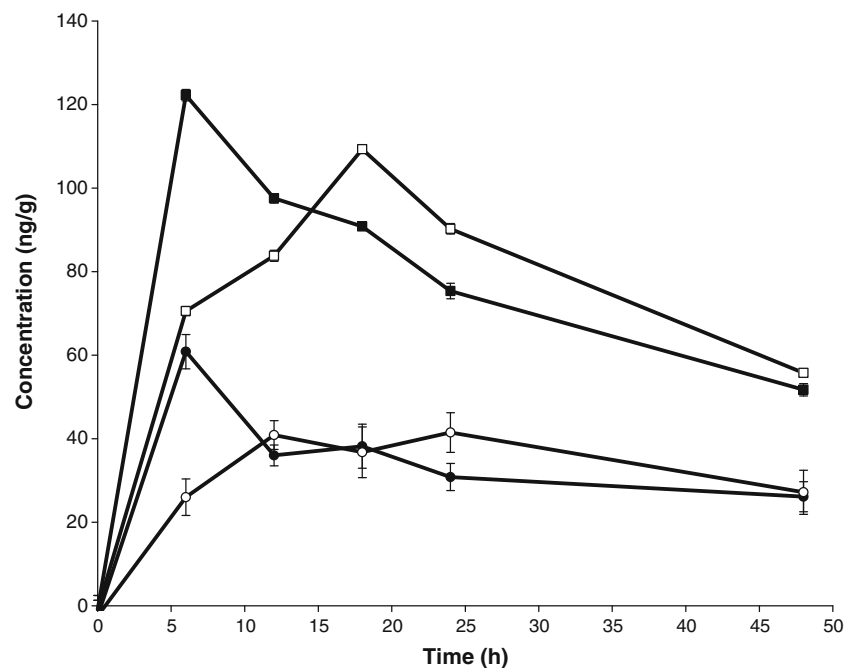
For selenium speciation, a similar calculation procedure was employed. In this case, every point in the chromatogram at all measured masses (here including mass 75 for a better definition of the SeH/Se factor using ^{74}Se added post-column) was subjected to multiple linear regression. A sixth theoretical pattern for natural abundance arsenic (100% ^{75}As) had to be included in Eq. (5) as this element could be present in some of

Fig. 5 Concentrations of selenium vs. time in serum (squares) and red blood cells (circles) for ^{nat}Se (a) and ^{77}Se (b) when administering inorganic selenium (black symbols) or organic selenium (white symbols). Error bars indicate standard uncertainties. (a) Natural abundance selenium. (b) ^{77}Se -labelled

a Natural abundance selenium



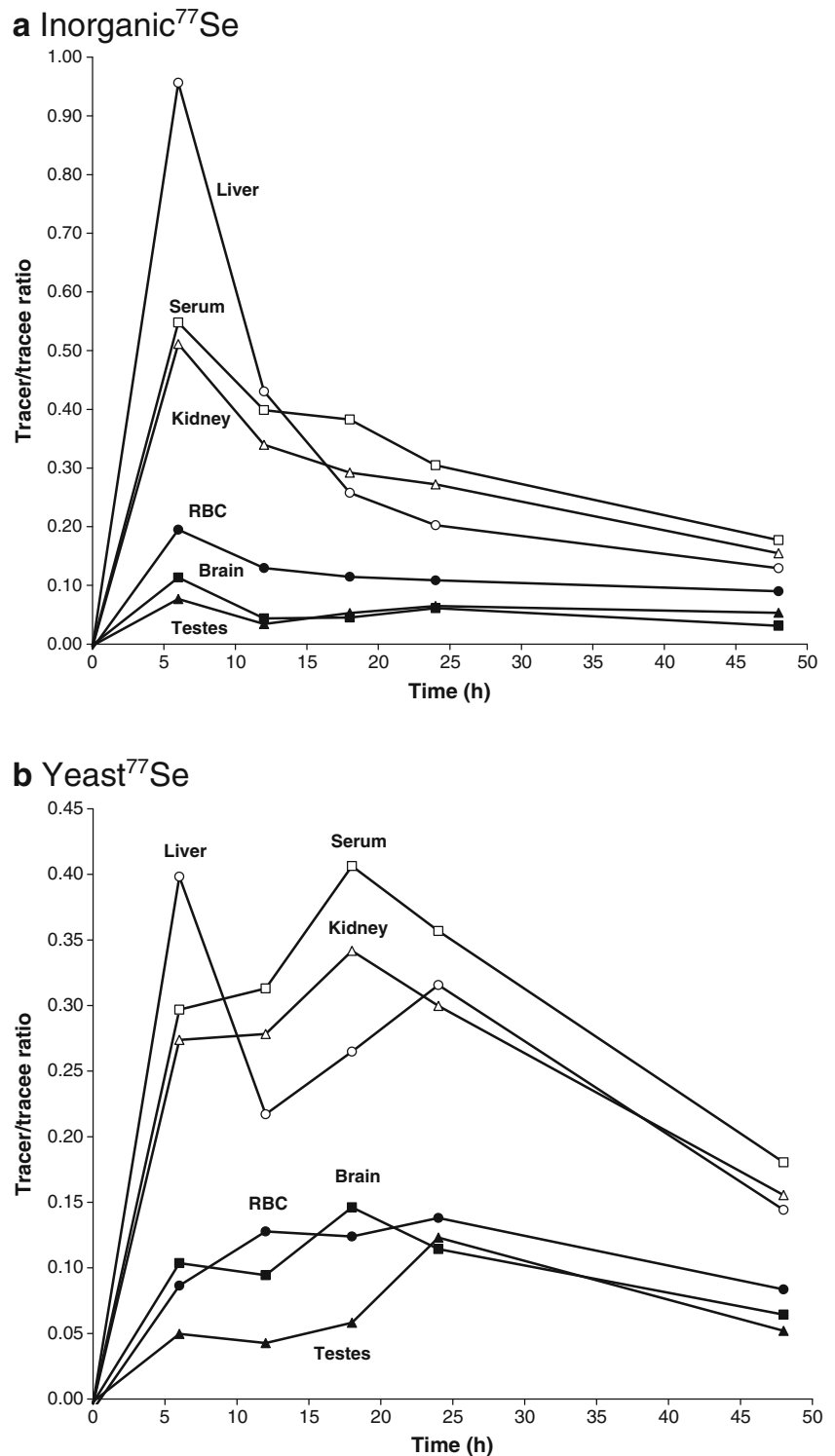
b ^{77}Se -labelled



the samples analysed such as urine. The square sum of residuals was calculated for every point in the chromatogram and the sum of all squared residuals for the chromatogram used in the optimisation procedure. For each chromatogram, an independent optimisation was performed. A typical chromatogram for serum or urine speciation contained *ca.* 800–900 data

points obtained every 2 s at 10 different masses (0.2 s integration time per mass). In all cases (11 urine samples and 11 serum samples) the optimised mass bias and hydride values were very similar and close to those obtained by total analysis. For example, Fig. 3 shows the optimised values for the BrH/Br and the SeH/Se factors together with the mass bias factors *k*

Fig. 6 Tracer/tracee ratios ($^{77}\text{Se}/^{\text{nat}}\text{Se}$) for inorganic selenium administration (a) and organic selenium (b). Tissues indicated are liver, serum, kidney, rbc, brain and testes. (a) Inorganic ^{77}Se . (b) Yeast ^{77}Se



calculated for the 11 serum samples. As can be observed, reasonable and reproducible values were obtained by the internal multiple linear regression procedure. For the BrH/Br factor the average value was 0.117 ± 0.001 (1 s) which is very close to that obtained for the 132 samples for total selenium (0.128). For the SeH/Se factor, the average value was 0.021 ± 0.004 (1 s) which was also close to the selenium hydride factor calculated for the 132 samples analysed for total selenium (0.030). In conclusion, the multiple linear regression procedure applied with internal optimisation of the hydride factors and mass bias provided chemically meaningful results of the mass bias and hydride factors. Finally, the average mass bias factor k calculated for the 11 chromatograms was -0.027 ± 0.001 (1 s) which was also similar to the best fit value for the 132 samples of $k = -0.025$.

The only problem observed with this calculation procedure was due to spectral skew. For some masses the fit was limited by the sequential nature of the quadrupole measurements. For example, Fig. 4a shows the experimental and the fitted chromatogram at mass 80 together with the residuals calculated in one of the serum chromatograms. As can be observed, during peak elution, a series of positive/negative residuals are obtained and this is clearly seen for the SePP1 peak at *ca.* 7.5 min. The small differences in the times in which all masses are measured during peak elution (spectral skew) produced this trend of positive residuals before the peak and negative residuals after the peak. Anyway, the maximum value of the residuals (*ca.* 300 counts) was less than 1% of the absolute count values at this mass so the reconstructed chromatogram fitted very well to the measured chromatogram. Apart from these minor problems of spectral skew all chromatograms obtained at all masses could be reconstructed adequately by the proposed multiple linear regression procedure.

The variation of the contribution factors, x_j , with time are given in Fig. 4b for the same serum sample shown

in Fig. 4a. These contribution factors can be seen here as the sum of all intensities at the different masses that can be ascribed to a certain isotope pattern. As can be observed, a large peak between 2 and 3 min was ascribed to the natural abundance bromine pattern. Once the contribution of bromine is computed all other selenium patterns are free from spectral interferences and show the real contribution of each selenium pattern to the observed intensities.

For the calculation of the concentrations of ^{nat}Se and ^{77}Se we have only to divide, point by point, the contribution of the ^{nat}Se or ^{77}Se by the contribution of ^{74}Se added post-column. In that way we obtain the relative molar flow chromatogram shown in Fig. 4c where the first peak corresponds to GPX3 and other unknown selenium species, and the second peak to SePP1 and the third small peak to SeAlb. The y -axis represents the ratio of molar flows $^{nat}\text{Se}/^{74}\text{Se}$ or $^{77}\text{Se}/^{74}\text{Se}$. As we know the molar flow of ^{74}Se (added post-column), we can calculate the molar flows of the other selenium isotopic patterns. Finally, the integration of the molar flow chromatograms provides directly the mols of each selenium pattern in each peak. So, pattern specific quantitative information can be obtained by this procedure. Obviously, the tracer/tracee ratio can be obtained for each peak obtaining species-specific metabolic data.

Time-related selenium incorporation and elimination in tissues

To test the mathematical procedure developed, a very simple metabolic experiment was carried out. Five male Wistar rats were fed $10.8 \mu\text{g}$ of ^{77}Se in the form of Se(IV) in water and another five $10.0 \mu\text{g}$ of ^{77}Se in the form of selenized yeast in a suspension. An untreated rat was used as control. Solid

Table 6 Results for selenium speciation in serum obtained for the experiments with ^{77}Se in inorganic and organic (yeast) forms. Concentrations in ng/g

Fraction	Control		6 h		12 h		18 h		24 h		48 h	
	^{nat}Se	^{77}Se	^{nat}Se	^{77}Se	^{nat}Se	^{77}Se	^{nat}Se	^{77}Se	^{nat}Se	^{77}Se	^{nat}Se	^{77}Se
Inorganic ^{77}Se												
GPX3	27	nd	53	30	32	6	35	4	46	7	50	7
SePP1	127	nd	124	85	71	48	106	55	132	52	149	28
SeAlb	6	nd	17	13	12	4	11	4	14	4	17	4
Total	160	–	193	128	115	58	151	63	191	63	216	39
Yeast ^{77}Se												
GPX3	–	–	65	16	64	13	68	12	51	11	50	7
SePP1	–	–	139	54	145	64	143	82	135	60	162	30
SeAlb	–	–	20	9	22	7	18	7	16	7	17	4
Total	–	–	224	79	232	85	229	100	202	78	229	42

samples were microwave digested, while liquid samples were diluted and all samples measured by ICP-MS as indicated in the procedures. Data on concentrations of ^{nat}Se and ^{77}Se as well as $^{77}\text{Se}/^{nat}\text{Se}$ (tracer/tracee ratios) could be obtained together with their standard uncertainties (from the multiple linear regression calculations). Tables 4 and 5 summarise all concentration results obtained for inorganic selenium (Table 4) and organic selenium (Table 5). All

results are expressed in ng/g on a wet weight basis except for serum and urine where a simple dilution with water and ^{74}Se spiking was performed. In order to better understand the results a graphic representation is more suitable. Figure 5 shows the data obtained for serum and red blood cells both for natural abundance selenium (Fig. 5a) and ^{77}Se enriched (Fig. 5b). As can be observed in Fig. 5a, the concentrations of natural abundance selenium are relatively constant with

Fig. 7 Tracer/tracee ratios ($^{77}\text{Se}/^{nat}\text{Se}$) for inorganic selenium administration (a) and organic selenium (b) for selenium species in serum. (a) Inorganic ^{77}Se . (b) Yeast ^{77}Se

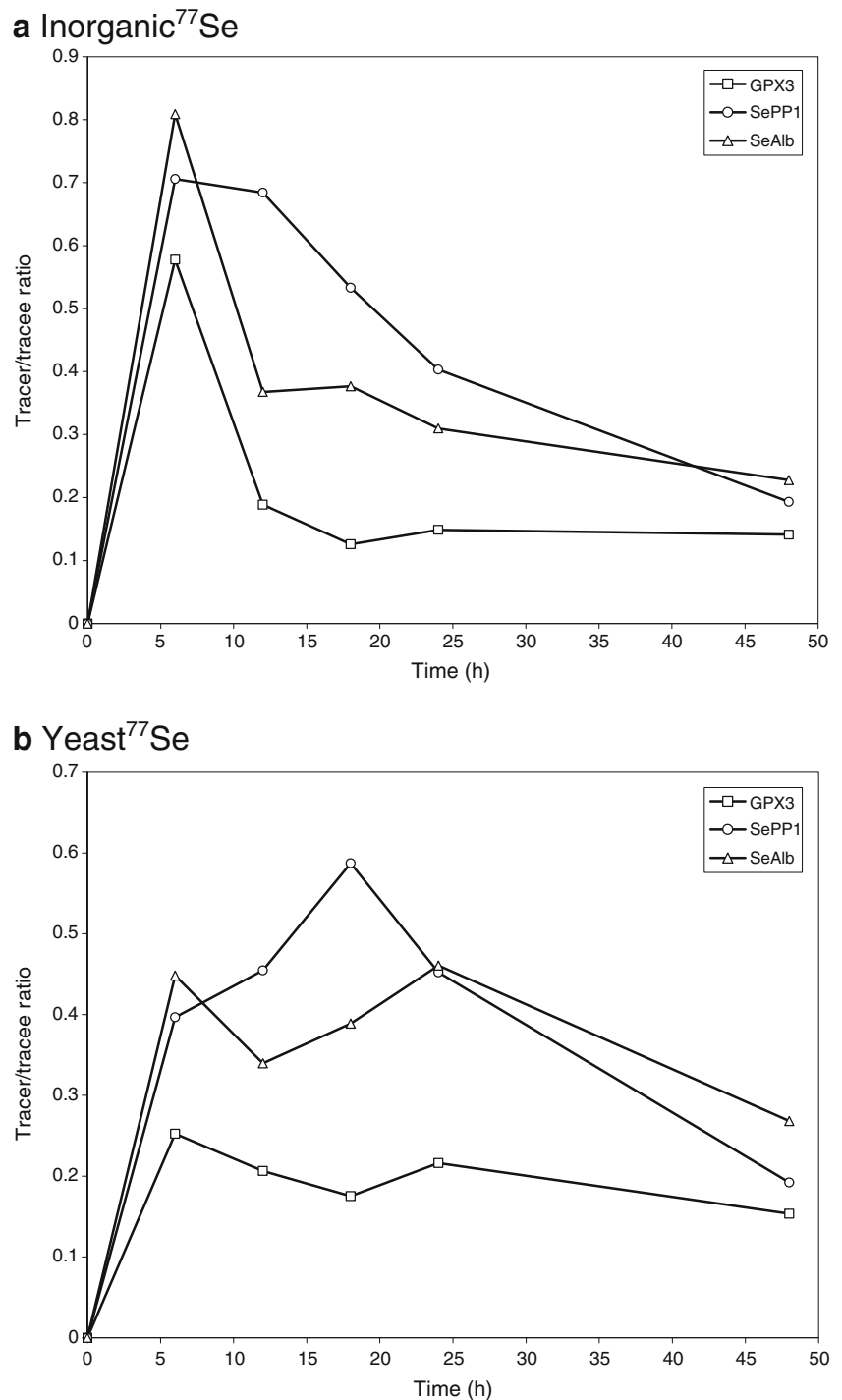
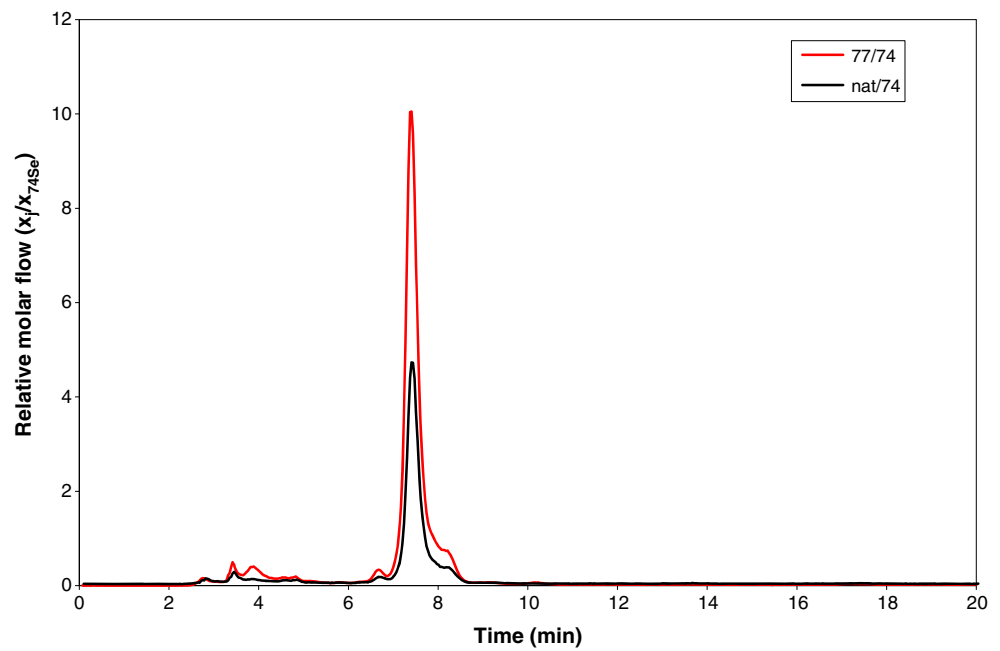


Fig. 8 Typical relative mass flow chromatogram of a urine sample (Yeast ^{77}Se administration after 18 h). Reverse phase chromatographic procedure, see the “Experimental” section



time for both samples and both forms of supplementation (inorganic and organic ^{77}Se). No corrections based on the weights of the rats were performed here. So, steady state conditions for natural abundance selenium seemed to have been achieved for this experiment. Similar results were obtained for all sample types. The results for labelled ^{77}Se are given in Fig. 5b. Here it can be observed that incorporation of inorganic ^{77}Se is progressing faster than for yeast ^{77}Se . Inorganic selenium peaks at 6 h while organic selenium peaks at 18 h. The results are similar for the other tissues. When comparing serum and red blood cells it is clear that the relative amount of ^{77}Se incorporated in serum is much higher than the relative incorporation in the red blood cells. However, these comparative incorporation

data is better seen as tracer/tracee ratios as these ratios should not be strongly affected by rat weight or biological variability between individuals.

Figure 6 shows the tracer/tracee ratios for selected tissues and inorganic selenium administration (Fig. 6a) or organic selenium administration (Fig. 6b). As can be observed, the time profiles for tissue incorporation are completely different for both selenium sources. Inorganic selenium is rapidly incorporated in all tissues (6 h) with a continuous decay afterwards. On the other hand, organic selenium peaks between 18 and 24 h except for the liver that shows a mixed behaviour with two peaks at 6 and 24 h. For both tracer forms, there is a distinct behaviour between liver, serum and kidney on the one

Table 7 Results for selenium speciation in urine

Type	Control		6 h		12 h		18 h		24 h		48 h	
	nat ^{74}Se	^{77}Se	nat ^{74}Se	^{77}Se	nat ^{74}Se	^{77}Se	nat ^{74}Se	^{77}Se	nat ^{74}Se	^{77}Se	nat ^{74}Se	^{77}Se
Inorganic ^{77}Se												
Peak 1	5.1	nd	8.1	28.4	10.8	32.4	32.5	64.8	19.3	45.3	22.5	19.1
Peak 2	21.8	nd	17.8	101.2	74.7	291.8	135.6	283.8	149.2	363.4	127.7	122.4
Total Se	26.9	nd	25.9	129.6	85.5	324.1	168.0	348.5	168.6	408.7	150.2	141.5
Yeast ^{77}Se												
Peak 1	–	–	22.7	75.3	9.0	17.9	24.7	54.6	43.0	111.7	17.3	11.9
Peak 2	–	–	144.7	403.5	77.8	55.4	242.0	503.4	252.9	437.3	57.7	30.2
Total Se	–	–	167.4	478.8	86.8	73.3	266.6	557.9	295.8	549.0	75.0	42.1

Peak 1 corresponds to the sum of all peaks between 2 and 5 min retention time. Peak 2 corresponds to the selenosugar plus the two small satellite peaks. Total selenium is the sum of peaks 1 and 2. Concentrations in ng/g

hand and RBC, brain and testes on the other hand. Much lower tracer/tracee ratios are obtained for these last three tissues.

It is not the objective of this work to discuss in detail selenium metabolism but to show that relevant metabolic results can be obtained easily by combining the double isotope approach with advanced data treatment methodologies. It is clear that a larger number of animals would be needed to conclude on the metabolic information.

Time related incorporation of selenium into serum proteins

For the study of selenium incorporation into serum proteins, the affinity procedure developed by Reyes *et al.* [2] was applied. As can be observed in Fig. 4c, three fractions were isolated by affinity chromatography. The first fraction corresponded to GPX3 and other non retained selenium compounds, the second fraction corresponded to SePP1 and the third fraction to SeAlb. Based on the relative molar flow chromatograms obtained for all samples, the concentrations of natural abundance selenium (^{nat}Se) and isotopically labelled selenium (^{77}Se) could be calculated for all three fractions. The results obtained are summarised in Table 6 both for inorganic ^{77}Se and organic (yeast) ^{77}Se respectively. The sum of all fractions should be similar to the total concentrations shown in Tables 4 and 5 for serum. Speciation recoveries (column recoveries) were, on average, $80\pm 16\%$ from those of total analysis.

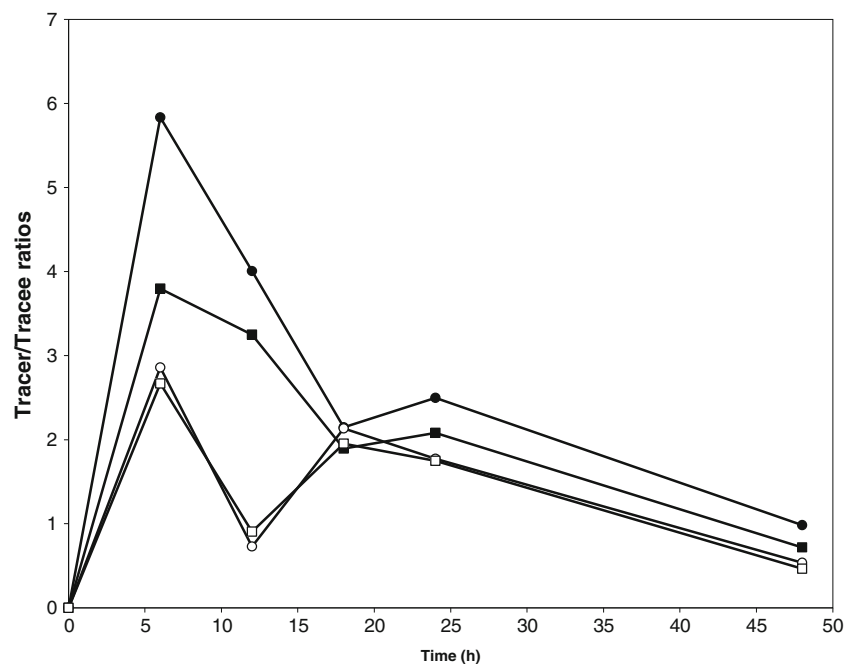
The tracer/tracee ratios for each selenium fraction and type of ^{77}Se label are shown in Fig. 7 for inorganic

^{77}Se (Fig. 7a) and yeast ^{77}Se (Fig. 7b). As can be observed, all selenoproteins show different tracer/tracee ratios and different apparent rates of synthesis and degradation. Fast turnover is observed for inorganic ^{77}Se administration while a slower turnover was observed for yeast ^{77}Se with SePP1 peaking after 18 h of administration and SeAlb with a double peak at 6 and 24 h. It is remarkable to observe that SePP1 has a synthesis–degradation profile similar to that of total selenium in the kidney (Fig. 6), while SeAlb (and perhaps also GPX3) has a synthesis–degradation profile similar to total selenium in liver (Fig. 6) for both ^{77}Se sources. This behaviour fits reasonably well with SePP1 being a transport protein synthesized primarily in the liver where albumin is also synthesized [20]. The liver takes up the selenium after gastrointestinal uptake and synthesizes SeAlb and SePP1 [21]. Both proteins enter the bloodstream and as SePP1 is the Se-transport protein it is selectively taken up by the kidney, thereby increasing the Se content of the organ, and the kidney utilizes the selenium from SePP1 to synthesize GPX3 [22, 23].

Time related urinary excretion of selenium

Figure 8 shows a typical reverse phase relative molar flow chromatogram for ^{nat}Se and ^{77}Se in urine. The main peak at *ca.* 7.5 min corresponds to the selenosugar [8, 9]. The other small peaks were not identified. All urine chromatograms obtained had the same profile with varying contribution from ^{nat}Se or ^{77}Se . It was decided to integrate the chromatograms in two parts. The first peak (peak 1) corresponded to

Fig. 9 Tracer/tracee ratios for the selenosugar peak (peak 2) in urine (circles) and for total selenium (squares). Yeast ^{77}Se is shown as white symbols and inorganic ^{77}Se as black symbols



the small peaks with retention times between 2 and 5 minutes. The second peak (peak 2) corresponded to the main selenosugar peak and the two small satellite peaks on both sides. The sum of all urine peaks could be compared with the results obtained for the total selenium concentrations found for the same urine samples to check for selenium recovery. The average recovery (column recovery) was 67% with a standard deviation of 13%. Also, the tracer/tracee ratios in the selenosugar peak (peak 2) for the two ^{77}Se sources could be calculated. The concentration results found are shown in Table 7 and the tracer/tracee ratios for peak 2 represented in Fig. 9 in comparison with the results for total selenium (Tables 4 and 5). As can be observed in Fig. 8, the tracer/tracee ratios for the selenosugar are close to those observed for total selenium in urine, particularly for the rats administered with yeast ^{77}Se . It is again remarkable that the synthesis–degradation profile obtained for the selenosugar is very similar to that obtained for total selenium in liver (Fig. 6) indicating that this organ is responsible for the synthesis of the selenosugar in agreement with the results of Ogra *et al.* [24].

Conclusion

The mathematical procedure developed here allows the fast and reliable study of selenium metabolism. The examples given here with only 11 rats should not be considered as a metabolic study but only to indicate that comprehensive total elemental and speciation information can be obtained by combining this dual isotope procedure [8, 9] with advanced data treatment in which all intensity data are treated simultaneously. This methodology should also be easily transferrable to human trials as no radioactivity is used and a single bolus dose of enriched selenium is employed.

Acknowledgements We would like to thank PharmaNord for supplying of the ^{77}Se enriched yeast, Marisa Fernández Sánchez for the supply of the ^{74}Se spike and Teresa Fernández and Agustín Brea from the Biotery of the University of Oviedo for their help regarding animal experiments. Funding from the Spanish Ministry of Science and Innovation through project number CTQ2009-12814 and the Education and Science Council of the Principado de Asturias (grant BP07-059) are gratefully acknowledged.

References

- Gammelgaard B, Jackson M, Gabel-Jensen C (2011) *Anal Bioanal Chem* 399:1743–1763
- Reyes LH, Marchante-Gayon JM, García Alonso JI, Sanz-Medel A (2003) *J Anal At Spectrom* 18:1210–1216
- Reyes LH, Marchante Gayon JM, García Alonso JI, Sanz-Medel A (2003) *J Anal At Spectrom* 18:11–16
- Jitaru P, Goenaga-Infante H, Vaslin-Reimann S, Fiscaro P (2010) *Anal. Chim Acta* 657:100–107
- Jitaru P, Roman M, Cozzi G, Fiscaro P, Cescon P, Barbante C (2009) *Microchim Acta* 166:319–327
- Jitaru P, Prete M, Cozzi G, Turetta C, Cairns W, Seraglia R, Traldi P, Cescon P, Barbante C (2008) *J Anal At Spectrom* 23:402–406
- Jitaru P, Cozzi G, Gambaro A, Cescon P, Barbante C (2008) *Anal Bioanal Chem* 391:661–669
- González Iglesias H, Fernández Sánchez M, Rodríguez-Castrillón JA, García Alonso JI, López Sastre J, Sanz-Medel A (2009) *J Anal At Spectrom* 24:460–468
- González Iglesias H, Fernández Sánchez M, García Alonso JI, Sanz-Medel A (2007) *Anal Bioanal Chem* 389:707–713
- Suzuki KT, Tsuji Y, Ohta Y, Suzuki T (2008) *Toxicol Appl Pharmacol* 227:76–83
- Suzuki KT, Ohta Y, Suzuki N (2006) *Toxicol Appl Pharmacol* 217:51–62
- Suzuki KT, Somekawa L, Kurasaki K, Suzuki N (2006) *J Health Sci* 52:590–597
- Suzuki KT, Somekawa L, Suzuki N (2006) *Toxicol Appl Pharmacol* 216:303–308
- Suzuki KT, Doi C, Suzuki N (2006) *Toxicol Appl Pharmacol* 217:185–195
- Rodríguez-Castrillón JA, Reyes LH, Marchante-Gayon JM, Moldovan M, Alonso JIG (2008) *J Anal At Spectrom* 23:579–582
- Larsen EH, Sloth JJ, Hansen M, Moesgaard S (2003) *J Anal At Spectrom* 18:310–316
- Sloth JJ, Larsen EH (2000) *J Anal At Spectrom* 15:669–672
- Sloth JJ, Larsen EH, Bugel SH, Moesgaard S (2003) *J Anal At Spectrom* 18:317–322
- Berglund M, Wieser ME (2011) *Pure Appl Chem* 83:397–410
- Schomburg L, Schweizer U, Holtmann B, Flohe L, Sendtner M, Kohrle J (2003) *Biochem J* 370:397–402
- Kato T, Read R, Rozga J, Burk RF (1992) *Am. J Physiol* 262:G854–G858
- Avissar N, Ornt DB, Yagil Y, Horowitz S, Watkins RH, Kerl EA, Takahashi K, Palmer IS, Cohen HJ (1994) *Am. J Physiol* 266:C367–C375
- Hill KE, Zhou JD, McMahan WJ, Motley AK, Atkins JF, Gesteland RF, Burk RF (2003) *J Biol Chem* 278:13640–13646
- Ogra Y, Ishiwata K, Takayama H, Aimi N, Suzuki KT (2002) *J Chromatogr B Analyt Technol Biomed Life Sci* 767:301–312